

PHYSICAL PROPERTIES AND PHASE DIAGRAM OF THE MAGNETIC COMPOUND $\text{Cr}_{0.26}\text{NbS}_{1.74}$ AT HIGH PRESSURES

V. A. Sidorov^a, A. E. Petrova^a, A. N. Pinyagin^{a,b},

N. N. Kolesnikov^c, S. S. Khasanov^c, S. M. Stishov^{a}*

^a Institute for High Pressure Physics, Russian Academy of Sciences
142190, Troitsk, Moscow, Russia

^b Moscow Institute of Physics and Technology
141700, Dolgoprudny, Moscow Region, Russia

^c Institute of Solid State Physics, Russian Academy of Sciences
142432, Chernogolovka, Moscow Region, Russia

Received October 15, 2015

We report a study of magnetic, electrical, and thermodynamic properties of a single crystal of the magnetic compound $\text{Cr}_{0.26}\text{NbS}_{1.74}$ at ambient and high pressures. Results of the measurements of magnetization as a function of temperature reveal the existence of a ferromagnetic phase transition in $\text{Cr}_{0.26}\text{NbS}_{1.74}$. The effective number of Bohr magnetons per Cr atom in the paramagnetic phase of $\text{Cr}_{0.26}\text{NbS}_{1.74}$ is $\mu_{\text{eff}} \approx 4.6\mu_B$, which matches the literature data for $\text{Cr}_{1/3}\text{NbS}_2$. Similarly, the effective number of Bohr magnetons per Cr atom in the saturation fields is rather close in both substances and corresponds to the number of magnetons in the Cr^{+3} ion. In contrast to the stoichiometric compound, $\text{Cr}_{0.26}\text{NbS}_{1.74}$ does not show a metamagnetic transition, that indicates the lack of a magnetic soliton. A high-pressure phase diagram of the compound reveals the quantum phase transition at $T = 0$ and $P \approx 4.2$ GPa and the triple point situated at $T \approx 20$ K and $P \approx 4.2$ GPa.

DOI: 10.7868/S0044451016060109

same crystal structure as $\text{Cr}_{1/3}\text{NbS}_2$ but somewhat different chemical composition.

1. INTRODUCTION

The magnetic compound Cr_xNbS_2 is a product of intercalation of the hexagonal 2H NbS_2 crystal structure with Cr ions. The value of x in the above formula can vary from 0.25 to 0.33 [1]. The reported temperature T_c of the phase transition to the magnetic phase in $\text{Cr}_{1/3}\text{NbS}_2$ varies from 115 to 160 K [2–5]. It was shown recently [6, 7] that a magnetic ordering in $\text{Cr}_{1/3}\text{NbS}_2$ results in a helical spin structure with the wave vector directed along the c -axis. A magnetic soliton lattice is formed in $\text{Cr}_{1/3}\text{NbS}_2$ in magnetic fields applied along the ab plane [6, 7] due to the structural anisotropy, as was predicted in Ref. [8]. The magnetic phase diagram is well described in Ref. [3]. Applying a high pressure shows that the phase transition point in $\text{Cr}_{1/3}\text{NbS}_2$ decreases with pressure [9, 10]. In this paper, we report a high-pressure study of the resistivity and magnetic susceptibility of a single crystal of a material with the

2. EXPERIMENT

The crystals of Cr_xNbS_2 were grown by chemical vapor transport using iodine as the transport agent. Single crystals of sort of brittle flakes of irregular form with a linear size of about 3 mm and about 0.05 mm of thickness were obtained. A small as grown crystal sample (with size about 0.2 mm) was used for a full X-ray diffraction data collection on Oxford diffraction CCD diffractometer with MoK_α radiation and for a crystal structure refinement. A chemical analysis of the grown crystals was performed by an electron-probe microanalysis technique.

For further characterization of the crystals, their electrical resistivity, magnetization, and heat capacity were measured. Electrical measurements were done by a four-terminal ac method. The specific heat and magnetization were measured with a Quantum Design physical property measurement system (PPMS). The

* E-mail: sergei@hppi.troitsk.ru

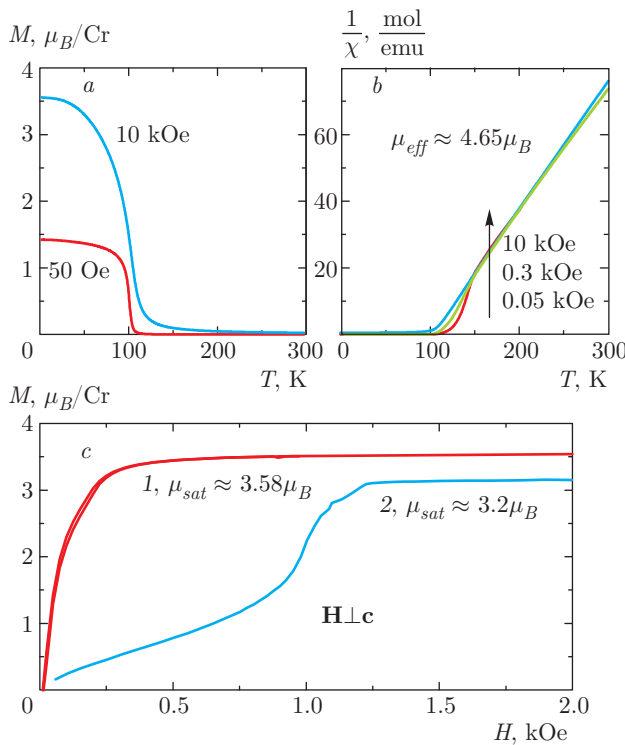


Fig. 1. (a) Temperature dependence of the magnetic moment of $\text{Cr}_{0.26}\text{NbS}_{1.74}$ in 50 Oe and 10 kOe magnetic fields. (b) Temperature dependence of the inverse magnetic susceptibility at different magnetic fields; the indicated effective magnetic moment per Cr atom is calculated from the linear part of the dependence. (c) Magnetic moment as a function of the applied magnetic field at 2 K for (1) $\text{Cr}_{0.26}\text{NbS}_{1.74}$ and (2) $\text{Cr}_{1/3}\text{NbS}_2$ from Ref. [3]; the indicated effective magnetic moments per Cr atom are calculated from the saturation magnetization

PPMS heat capacity module and vibration magnetometer were used. High pressures were created using a miniature toroid-type clamped device. A sample with a coil system for magnetic ac-susceptibility measurements and a sample for resistivity measurements was placed inside a Teflon capsule [11]. The capsule was inserted inside a toroid cell. Pressure was measured by monitoring the superconducting transition temperature of Pb located near the sample [11].

3. RESULTS AND DISCUSSION

A single-crystal X-ray analysis shows that the synthesized material belongs to the space group $P6_322$, Nb_3CoS_6 , hp20 structure type without a center of symmetry [5]. The structure refinement shows that the occupation of Cr atom positions is stoichiometric.

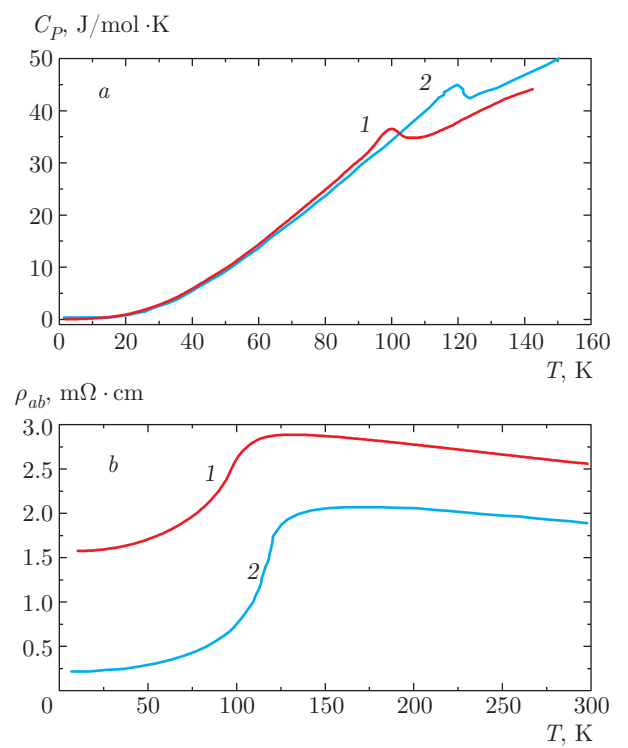


Fig. 2. (a) Temperature dependences of the (a) heat capacity and (b) resistivity for (1) $\text{Cr}_{0.26}\text{NbS}_{1.74}$, present data, and (2) $\text{Cr}_{1/3}\text{NbS}_2$, Ref. [3]

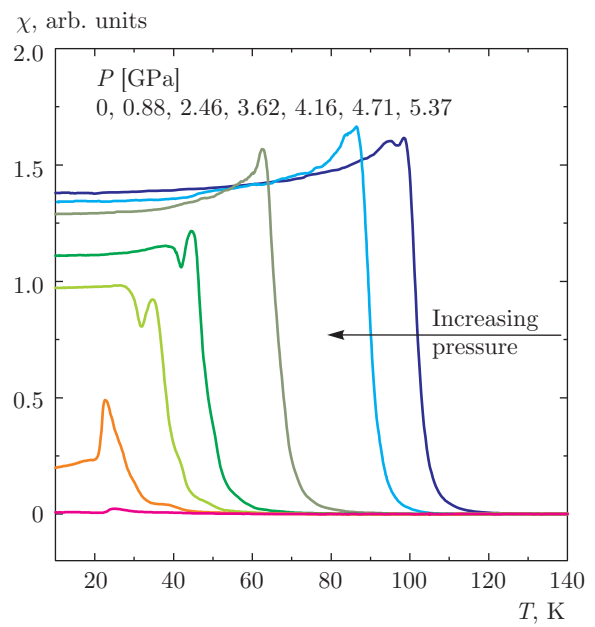


Fig. 3. Temperature dependence of ac susceptibility at different pressures for $\text{Cr}_{0.26}\text{NbS}_{1.74}$

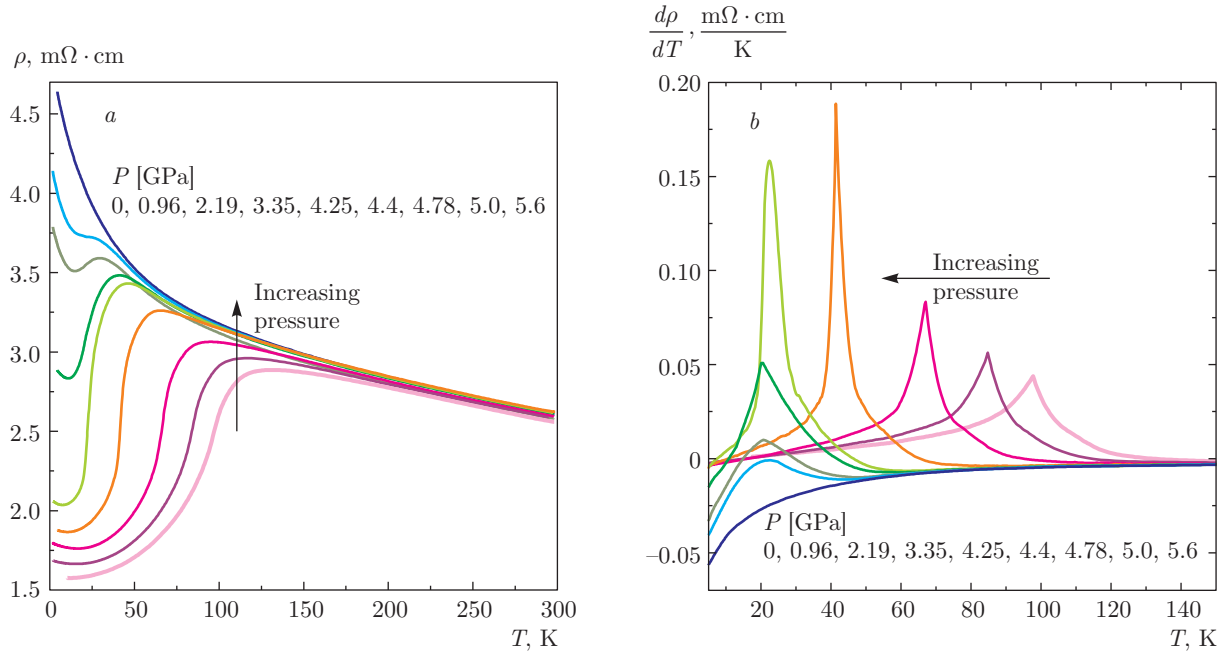


Fig. 4. (a) Resistivity and (b) its temperature derivative as functions of temperature at different pressures for $\text{Cr}_{0.26}\text{NbS}_{1.74}$

ric within 1 %. No deficit in the sulfur positions was found. The refinement resulted in values of the R -factors $R_1 = 0.019$ and $R_{wp} = 0.043$, quite comparable with data in [12] for the $P6_3$ space group. Hence, the choice of a lower symmetry in Ref. [12] did not improve the structure description. The unit-cell parameters obtained as $a = 5.744(1)$ Å and $c = 12.132(2)$ Å, are in principal agreement with the data in [3–5], although the c -parameter seems to be slightly higher. However, a chemical analysis of big crystals used for physical measurements, performed by an electron-probe microanalysis technique, gives a composition close to $\text{Cr}_{0.26}\text{NbS}_{1.74}$. Therefore, these crystals probably have an excessive amount of Nb, which is situated in Cr positions, and hence a deficit of Cr. As a result, a defect structure with Cr atoms randomly distributed over the corresponding positions is formed. A decreased concentration of Cr atoms should influence some physical properties of the material. In particular, one might expect the lower Curie temperature and saturation magnetic field of the grown crystals compared with those of standard material, which appears to be true.

The results of measurements of the magnetization, resistivity, and heat capacity and the available data on the stoichiometric $\text{Cr}_{1/3}\text{NbS}_2$ are displayed in Figs. 1 and 2. Figure 1a, describing behavior of the magnetic moment as a function of temperature, reveals the existence of a ferromagnetic phase transition in our ma-

terial. An effective number of Bohr magnetons per Cr atom in the paramagnetic phase of $\text{Cr}_{0.26}\text{NbS}_{1.74}$ is $\mu_{\text{eff}} \approx 4.6\mu_B$ (Fig. 1b), which matches the literature data for $\text{Cr}_{1/3}\text{NbS}_2$. The Sommerfeld coefficient γ and the Debye temperature T_D , estimated from heat capacity data (Fig. 2a), are $\gamma = 8.68 \text{ mJ}\cdot\text{mol}^{-1}\cdot\text{K}^{-2}$ and $T_D \approx 415$ K. Our value of γ strongly differs from the value cited in Ref. [3] for $\text{Cr}_{1/3}\text{NbS}_2$. But this difference probably results from a choice of the molecular unit used in calculations.

Remarkably, the comparison of the data shown in Fig. 2 agrees with our expectations. The Curie temperature is lower and the resistivity is higher in $\text{Cr}_{0.26}\text{NbS}_{1.74}$ than in the standard material. But these appear to be just a quantitative feature. A qualitative difference is seen in Fig. 1c, where the magnetizations of both materials are shown. The magnetization curve of $\text{Cr}_{1/3}\text{NbS}_2$ depicts a metamagnetic behavior, most probably connected with the transition from the helical to magnetic soliton lattice [6], whereas the magnetization of $\text{Cr}_{0.26}\text{NbS}_{1.74}$ does not contain such a feature. Surprisingly, the metamagnetic transition was not observed in the stoichiometric $\text{Cr}_{1/3}\text{NbS}_2$ in recent publication [12]. All this might imply that the helical spin structure in the compounds under consideration, if it does exist, is rather fragile and not always forms a soliton lattice. We note that even small magnetic fields destroy characteristic features of the magnetic phase

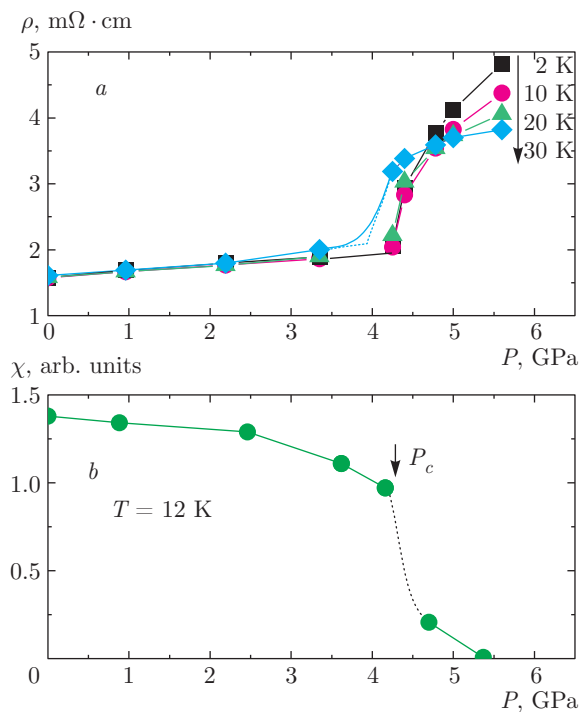


Fig. 5. (a) Pressure dependences of the (a) resistivity at different temperatures and (b) ac susceptibility at the temperature 12 K for $\text{Cr}_{0.26}\text{NbS}_{1.74}$

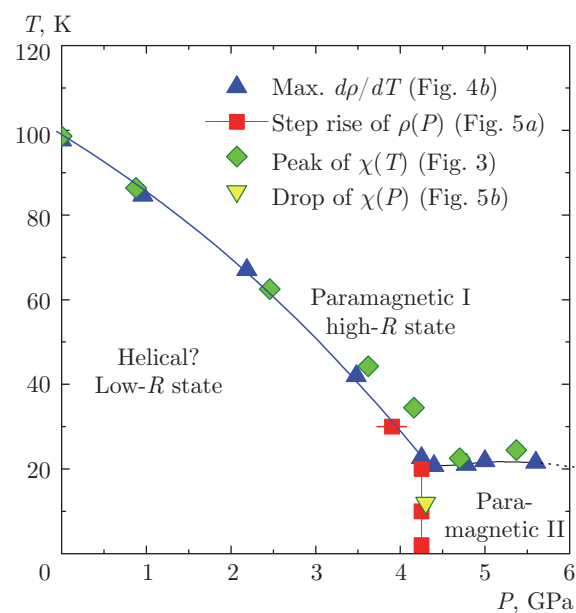


Fig. 6. Phase diagram of $\text{Cr}_{0.26}\text{NbS}_{1.74}$, constructed from the susceptibility and resistivity data (Figs. 4 and 5)

transitions observed in the ac susceptibility measurements (Fig. 3).

It is worth noting that the effective number of Bohr magnetons per Cr atom in the saturation fields is rather close in both substances and corresponds to the number of magnetons in the Cr^{+3} ion (see Fig. 1c) [13].

We next proceed to the high-pressure experiment.

Figures 3 and 4 illustrate behavior of the ac magnetic susceptibility χ and the resistivity ρ as functions of temperature at different pressures. The ac magnetic susceptibility χ in Fig. 3 looks typical for ferromagnets, the peak splitting being most probably due to two slightly different domains existing in the sample. The resistivity curves in Fig. 4a clearly demonstrate a transition to the state with a negative temperature coefficient in the magneto-ordered phase at high pressures. We note that this unusual resistivity behavior for a metal is also seen in the paramagnetic phase even at ambient pressure (see Fig. 2 and also Ref. [3]).

Using the data displayed in Figs. 3–5, we are able to construct a phase diagram of $\text{Cr}_{0.26}\text{NbS}_{1.74}$ at high pressures (Fig. 6). Significant features of the phase diagram in Fig. 6 are the quantum phase transition at $T = 0$ and $P \approx 4.2$ GPa and the triple point situated at $T \approx 20$ K and $P \approx 4.2$ GPa. The nature of the phase transition between the helical and paramagnetic phase II is not clear. Here, the steep rise of the resistivity in a limited range of pressure probably suggests a first-order phase transition. This circumstance puts certain limitations on characters of the helical-paramagnetic I and paramagnetic I-II phase transitions. But a detail discussion of this subject would now be premature.

4. CONCLUSION

Crystals of the nonstoichiometric magnetic compound $\text{Cr}_{0.26}\text{NbS}_{1.74}$ were grown by the chemical vapor transport method. A study of magnetic, electrical, and thermodynamic properties of a single crystal of the material at ambient and high pressures was performed. The results of measurements of the magnetization as a function of temperature reveal the existence of a ferromagnetic phase transition in $\text{Cr}_{0.26}\text{NbS}_{1.74}$. The effective number of Bohr magnetons per Cr atom in the paramagnetic phase of $\text{Cr}_{0.26}\text{NbS}_{1.74}$ is $\mu_{\text{eff}} \approx 4.6\mu_B$, which matches the literature data for $\text{Cr}_{1/3}\text{NbS}_2$. Similarly, the effective number of Bohr magnetons per Cr atom in the saturation fields is rather close in both substances and corresponds to the number of magnetons in the Cr^{+3} ion. In contrast to the stoichiometric compound, $\text{Cr}_{0.26}\text{NbS}_{1.74}$ does not show a metamagnetic transition, that indicates the lack of a magnetic soliton. A high-pressure phase

diagram of the compound reveals the quantum phase transition at $T = 0$ and $P \approx 4.2$ GPa and the triple point situated at $T \approx 20$ K and $P \approx 4.2$ GPa.

This work was supported by the RFBR (grant No. 15-02-02040), the RAS Program “Physics of novel materials and structures”, the Program of the Physics Department of RAS on Strongly Correlated Electron Systems, and the Program of the Presidium of RAS on Strongly Compressed Matter. A. E. P. (measurements and data analysis) is grateful to the Russian Science Foundation (grant No. 14-22-00093) for financial support.

REFERENCES

1. R. H. Friend, A. R. Beal, and A. D. Yoffe, *Phil. Mag.* **35**, 1269 (1977).
2. S. S. P. Parkin and R. H. Friend, *Phil. Mag. B* **41**, 65 (1980).
3. N. J. Ghimire, M. A. McGuire, D. S. Parker et al., *Phys. Rev. B* **87**, 104403 (2013).
4. T. Miyadai, K. Kikuchi, H. Kondo et al., *J. Phys. Soc. Jpn* **52**, 1394 (1983).
5. F. Hulliger and E. V. A. Pobitschka, *J. Sol. St. Chem.* **1**, 117 (1970).
6. Y. Togawa, T. Koyama, K. Takayanagi et al., *Phys. Rev. Lett.* **108**, 107202 (2012).
7. B. J. Chapman, A. C. Bornstein, N. J. Ghimire et al., *Appl. Phys. Lett.* **105**, 072405 (2014).
8. Y. A. Izyumov, *Uspekhi Fiz. Nauk* **144**, 439 (1984).
9. M. Mito, S. Tominaga, Y. Komorida et al., *J. Phys., Conf. Ser.* **215**, 012182 (2010).
10. M. Mito, T. Tajiri, K. Tsuruta et al., *J. Appl. Phys.* **117**, 183904 (2015).
11. A. E. Petrova, V. A. Sidorov, and S. M. Stishov, *Physica B* **359–361**, 1463 (2005).
12. V. Dyadkin, F. Mushenok, A. Bosak, D. Menzel, S. Grigoriev, P. Pattison, and D. Chernyshev, *Phys. Rev. B* **91**, 184205 (2015).
13. C. Kittel, *Introduction to Solid State Physics*, John Wiley & Sons, New York (1986).